



THE EFFECTIVENESS OF SEISMIC BUILDING CODE PROVISIONS ON REDUCING THE COLLAPSE RISK OF REINFORCED CONCRETE MOMENT FRAME BUILDINGS

Abbie B. Liel¹, Curt B. Haselton¹, and Gregory G. Deierlein²

ABSTRACT

This paper examines the effectiveness of building code provisions in mitigating seismic collapse risk by quantifying the collapse risk of four reinforced concrete frame structures. First, an existing and a new reinforced concrete moment frame building, designed for seismic conditions in coastal California, are compared to illustrate improvements in building code provisions over time, as measured in terms of reduction in collapse risk. This comparison is based on four-story reinforced concrete moment frame structures designed to be representative of a) pre-1970 non-ductile reinforced concrete construction and b) modern, ductile reinforced concrete construction. A second group of four-story reinforced moment frame structures is also considered, including modern code-conforming a) special, b) intermediate, and c) ordinary moment frames. These structures are designed for three different sites and the strength and detailing requirements are consistent with what is permitted for each site's seismic hazard. From analysis of these structures, the uniformity of safety provided by seismic building code provisions across regions of varying seismicity is evaluated.

Keywords: reinforced concrete, building code, collapse, safety, nonlinear simulation

INTRODUCTION

Recent developments in earthquake engineering research have enabled simulation of structural collapse under seismic loading, providing quantitative measures of collapse risk. Using these new tools, this paper examines the seismic collapse risk of reinforced concrete (RC) frame structures in the U.S. This comparison includes both modern and older existing structures designed for high seismic areas in California, as well as modern code-conforming structures designed for regions of lower seismicity in the central and eastern U.S. Employing the methodology of performance-based earthquake engineering, as developed by the Pacific Earthquake Engineering Research (PEER) Center, each structure is analyzed using nonlinear dynamic analyses to capture the important failure modes and collapse behavior. This probabilistic collapse assessment incorporates uncertainty in ground motions as well as structural behavior and modeling.

METHODOLOGY

This evaluation of reinforced concrete moment frame structures is based on the PEER performance-based earthquake engineering (PBEE) methodology which provides a framework for relating ground motion intensity (intensity measure, or IM) to the structural response (termed engineering demand

¹ Ph.D. Candidate, Dept. of Civil and Environmental Engineering, Stanford University, Stanford, CA 94305

² Professor, Dept. of Civil and Environmental Engineering, Stanford University, Stanford, CA 94305 (ggd@stanford.edu)

parameter, or EDP) through analytical models and structural simulation, and extends to loss estimation (Deierlein 2004). The application of the PEER methodology presented here focuses on collapse prediction and consists of inelastic dynamic analysis to directly simulate sidesway collapse.

Simulation of global sidesway collapse is based on the Incremental Dynamic Analysis (IDA) technique (Vamvatsikos and Cornell, 2003). The basic process of this technique is as follows: (a) a strong ground motion is selected and scaled to a specified ground motion intensity, such as spectral acceleration at the first mode period, (b) the peak response quantity, such as peak interstory drift ratio (IDR), is recorded and associated with the specified earthquake intensity, (c) steps (a) – (b) are repeated by scaling up the intensity of the input ground motion until the building becomes dynamically unstable and a collapse occurs, and finally (d) steps (a)-(c) are repeated for additional ground motions. In this study, the IDA analyses are based on a set of 22 pairs of recorded ground motions, each with two orthogonal components.³ These ground motions were selected to represent large earthquakes with moderate fault-rupture distances (i.e., non near-field conditions). The intensity measure used is the spectral acceleration at $T = 1$ sec, which is close to the fundamental period of the RC SMF building considered in this study; for simplicity, this same period was also used in the analyses of the other buildings.

Element deterioration and failure modes that cannot be directly simulated in the analysis are incorporated in the collapse assessment through damage analysis, which combines Engineering Demand Parameters (e.g., drift ratios) with fragility curves to evaluate the likelihood of other collapse modes. Loss of vertical load carrying capacity (LVCC) in shear critical reinforced concrete columns is an example of a deterioration mode which is incorporated through such a post-processing approach, as opposed to directly in the structural simulation.

After assessment through IDA, the collapse capacities can be plotted as a cumulative distribution function (CDF) representing the probability of collapse as a function of ground motion intensity (e.g., probability of collapse given the ground motion's spectral acceleration at 1 second). This process accounts only for uncertainty in response associated with variations in the ground motion records. In addition to these, the variation in response due to uncertainties in the structural properties and the analysis model must be considered. Termed the “modeling uncertainties”, these are incorporated in the procedure through a FOSM (First-Order Second Moment) probabilistic analysis.

Collapse safety can be quantified in several ways. One option is to express the conditional probability of collapse at a specified ground motion intensity level, e.g., the probability of collapse at the maximum considered earthquake (MCE) intensity. An alternative and more complete interpretation is to express collapse safety in terms of a mean annual frequency (MAF) of collapse. The MAF of collapse is obtained by integrating the collapse CDF with the ground motion hazard curve for a specified site. These metrics provide measures by which relative collapse safety of structures may be examined.

STRUCTURAL DESIGNS

Four buildings were designed and analyzed in this study, each of which has the same footprint and elevation geometry. Two of these structures were designed for a high seismic region, with member sizing and detailing (1) according to the 1967 Uniform Building Code (UBC) (ICBO 1967), and (2) according to the special moment frame requirements of the 2003 International Building Code (IBC) (ICC 2003). Figure 1 shows the plan and elevation of the 1967 space frame building. The 2003 special moment frame (SMF), ordinary moment frame (OMF), and intermediate moment frames (IMF) have the same layout, but are designed as perimeter frame systems. The designs are intended to represent

³ This is the basic Far-Field ground motion set selected by Haselton and Kircher as part of an Applied Technology Council project, ATC-63. These records were selected without consideration of epsilon, a measure of spectral shape which has been shown to have a significant impact on collapse capacity (Baker and Cornell 2005). Selecting for high epsilon, as is appropriate for rare ground motions at sites in California, has been found to increase median collapse capacity by about 40% for frame structures (Haselton et al. 2007, Goulet et al. 2006).

typical design practice, rather than code minimum design, including modest amounts of overstrength that reflect common practice.

The 1967 design represents typical non-ductile reinforced concrete construction prior to the institution of ductile detailing requirements in the UBC for high seismic areas. The 2003 design is a modern code-conforming design. Both are designed for a site in the Los Angeles area, where the maximum considered earthquake corresponds to $S_a(T = 1.0\text{sec}) = 0.90g$ and the site is not in a near-fault region (Goulet et al. 2006, Haselton et al. 2007). The 2003 SMF structure has perimeter frame columns ranging in size from 24 in. x 28 in. to 30 in. x 40 in. (610 x 710 mm to 760 to 1010 mm); beams are 32 to 42 in. (810 to 1070 mm) deep. The SMF design was controlled by strength, the strong column-weak beam requirement, joint shear capacity provisions, and somewhat by drift limitations (Haselton et al. 2007; ICC 2003). The 1967 space frame design has square columns, varying in dimension from 20 to 24 in. (510 to 610mm), and beams with depths between 20 to 26 in. (510 to 660 mm). The design was controlled by strength demands as the 1967 code has no strong column-weak beam or joint requirements (ICBO 1967).

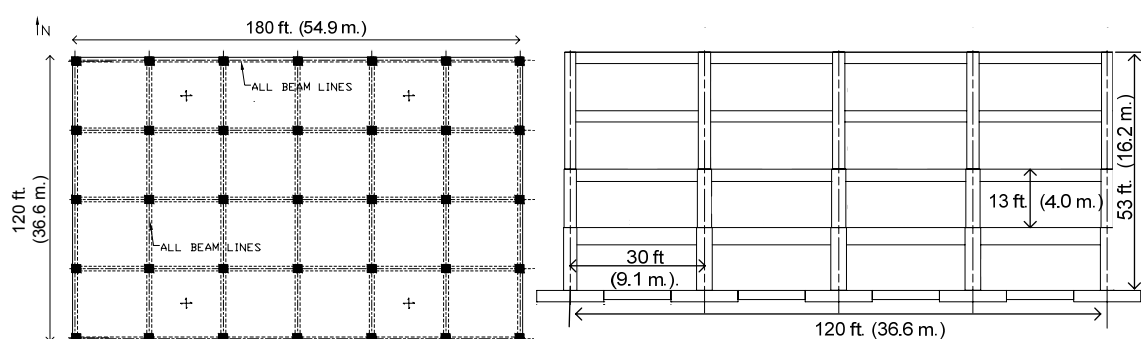


Figure 1. Plan and elevation (N-S) of four-story office building.

The ordinary and intermediate moment frames are designed according to the 2003 IBC and are designed for sites with maximum considered earthquakes corresponding to $S_a(T=1.0\text{sec}) = 0.19g$ and $S_a(T=1.0\text{sec}) = 0.32g$, respectively. The ordinary moment frame (OMF) has a design base shear coefficient of 0.045g (approximately one-half the SMF) and is controlled by member (beam-column) strength. Columns range in size from 20 in. x 22 in. to 28 in. x 28 in. (510 x 560mm to 710 x 710mm) and beams are between 20 and 26 in. (510 to 660mm) in depth. The IMF has the same member sizes and longitudinal reinforcement as the OMF, but with higher levels of detailing. In particular, columns and beams of the IMF have more closely spaced hoops, to comply with the element shear capacity design requirements (ICC 2003).

COLLAPSE MODELING OF RC FRAMES

Deterioration and Collapse Modes

Collapse evaluation first requires the identification of all deterioration modes that could lead to local or global structural collapse. Figure 2 shows the plan and elevation of the perimeter frame structures, with markers (A to F) referring to specific structural components whose associated deterioration modes are summarized Table 1. In addition to describing the key aspects of the behavior that lead to deterioration, Table 1 indicates the availability and maturity of models to assess these various deterioration modes. The following four figures and tables are after Deierlein et al. (2005).

These element deterioration modes may then be combined in potential collapse scenarios, as summarized in Table 2. The likelihood of the various collapse scenarios is judgmentally classified in Table 3 for the four categories of seismic moment frame systems considered in this paper. As indicated, the more stringent detailing and capacity design provisions for modern intermediate and special frames reduce the number of likely collapse scenarios for these systems. For example,

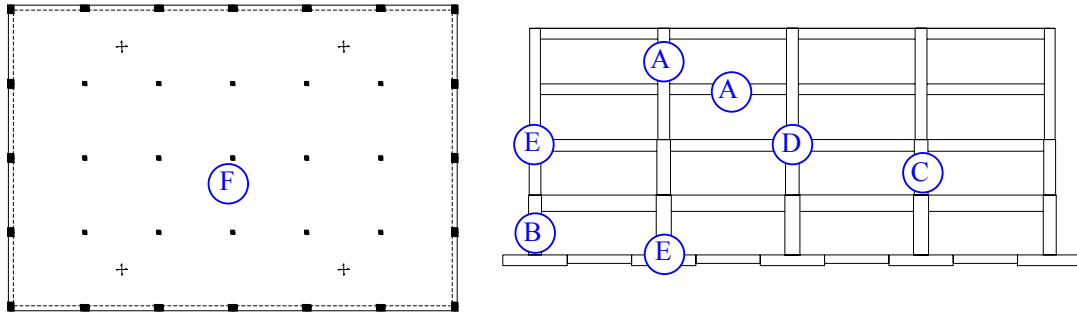


Figure 2. Reinforced concrete frame building plan and elevation views, show possible deterioration modes (after Deierlein et al. 2005).

Table 1. Deterioration modes of RC frame elements (after Deierlein et al. 2005).

Deterioration Mode	Element	Behavior	Simulation Model Availability	Fragility Model Availability	Description
A	Beam-column	Flexural	4	NR	Concrete cracking Concrete spalling Reinforcing bar yielding Concrete core crushing Reinforcing bar buckling (incl. stirrup fracture) Reinforcing bar fracture
B	Beam-column	Axial compression	2	4	Concrete crushing, longitudinal bar yielding Stirrup rupture, longitudinal bar buckling
C	Beam-column	Shear Shear + Axial	1	4	Concrete shear cracking Transverse tie pull-out Possible loss of axial load carrying capacity
D	Joint	Shear	3	2	Panel shear failure
E	Reinforcing bar connection	Pull-out or Bond-slip	2	2	Reinforcing bar bond-slip or anchorage failure at joint Reinforcing bar lap-splice failure Reinforcing bar pull-out (especially at footings)
F	Gravity frame slab-column connection	Punching shear	2	3	Punching shear at slab-column connection Possible vertical collapse of slab

(*1) Model Maturity (0: Non existent, 1-5: 1 - low confidence to 5 - high confidence; NR - Not required; behavior can be simulated)

Table 2. Possible collapse scenarios of RC frame systems (after Deierlein et al. 2005).

(a) Sidesway collapse scenarios

Scenario	Element Deterioration Mode						Description
	A	B	C	D	E	F	
FS1							Beam and column flexural hinging, forming sidesway mechanism
FS2							Column hinging, forming soft-story mechanism
FS3							Beam or column flexural-shear failure, forming sidesway mechanism
FS4							Joint-shear failure, likely with beam and/or column hinging
FS5							Reinforcing bar pull-out or splice failure, leading to sidesway mechanism

(b) Vertical collapse scenarios

Scenario	Element Deterioration Mode						Description
	A	B	C	D	E	F	
FV1							Column shear failure, leading to column axial collapse
FV2							Column flexure-shear failure, leading to column axial collapse
FV3							Punching shear failure, leading to slab collapse
FV4							Failure of floor diaphragm, leading to column instability
FV5							Crushing of column, leading to column axial collapse; possibly from overturning effects

Table 3. Likelihood of collapse scenarios for RC frame structures (after Deierlein et al. 2005).

Systems	Sidesway Collapse					Vertical Collapse				
	FS1	FS2	FS3	FS4	FS5	FV1	FV2	FV3	FV4	FV5
SMF	H	L-M	L	L	L-M	L	L	L	L	L-M
IMF	H	M	L	M	M	L	L	L	M	L-M
OMF/ '67 Frame	H	H	H	H	H	M	H	M	M	M-H

H: High, M: Medium, L: Low

	Collapse mode not included in model, because occurrence is unlikely.
	Collapse scenario simulated in OpenSees.
	Collapse scenario incorporated through a combination of simulation and post-
	Collapse mode not accounted for to date.

assuming that the special seismic detailing is sufficient to prevent most modes of local loss in vertical load carrying capacity (e.g., shear followed by axial failure in RC columns, axial-flexural crushing of columns leading to axial failure, punching shear collapse of slab-column connections), the only likely collapse mode for special moment frame is assumed to be sidesway collapse due to the combined effects of P- Δ and flexural strength/stiffness deterioration of beam-columns. For the OMF and '67 designs, which lack capacity design provisions, most failure modes are possible, though some are judged to be more likely than others. Many of these locally initiated collapse modes cannot be simulated directly using common analysis tools.

Simulation of Structural Collapse

The response of each frame structure is simulated using the OpenSees software (PEER 2006) with the following modeling features (Figure 3a): beam-column elements with concentrated inelastic rotational hinges at each end, finite size beam-column joints that employ five concentrated inelastic springs to model joint panel distortion and bond slip at each face of the joint; and elastic semi-rigid foundation springs. Lumped plasticity phenomenological models are used in order to capture softening post-peak response, which is difficult to simulate using fiber-element type models. The seismic resisting lateral system is represented by a two-dimensional, four-bay frame model, which incorporates large deformation response including destabilizing P- Δ effects. For the perimeter systems, the strength and stiffness of the gravity framing is neglected, but the additional P- Δ effects are included.⁴

The inelastic hinge models for the beam-columns and beam-column joints are described by the monotonic trilinear backbone curve developed by Ibarra et al (2005). This backbone and associated hysteretic rules provide for versatile modeling of cyclic behavior (Figure 3b). An important aspect of this model is the negative stiffness associated with the post-peak response, which enables modeling of strain softening behavior associated with phenomena such as concrete crushing, and rebar buckling and fracture. The model also captures four basic modes of cyclic deterioration: strength deterioration of the inelastic strain hardening branch, strength deterioration of the post-peak strain softening branch, accelerated reloading stiffness deterioration, and unloading stiffness deterioration.

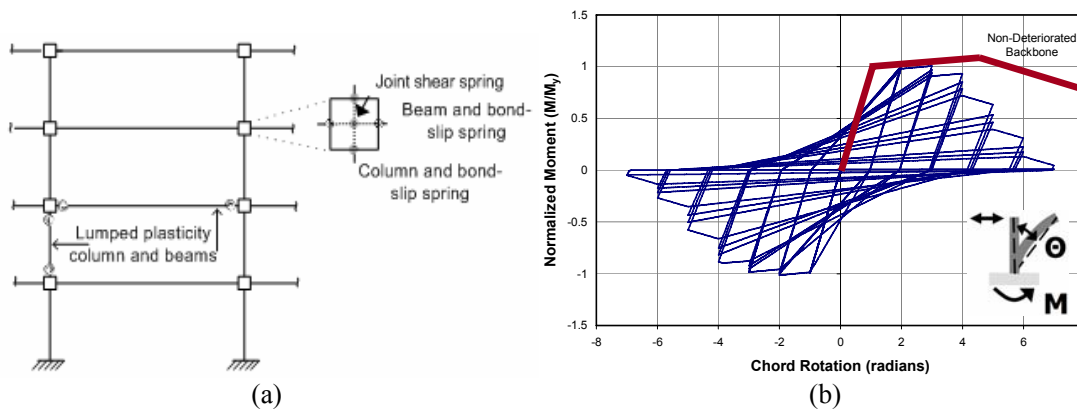


Figure 3. (a) Schematic diagram of OpenSees model; (b) Illustration of spring hinge model showing cyclic strength and stiffness degradation.

⁴ This assumption is conservative, and will impact the results for the weak/flexible OMF more than for the SMF.

The element hinge model requires specification of seven parameters to control both the monotonic and cyclic behavior of the element: M_y , θ_y , K_s , θ_{cap} , K_c , and two deterioration parameters (λ and c). The calibration of these parameters for reinforced concrete columns is part of a separate study (Haselton et al. 2006) of more than 250 columns from the PEER Structural Performance Database (PEER 2005). The element modeling parameters are highly dependent on the design and detailing requirements of beam, columns and joints. The differences in backbones for columns in the four types of RC frame structures considered are summarized in Figure 4. As shown, element models for non-ductile columns found in the OMF and '67 frames include a smaller plastic rotation capacity ($\theta_{cap,pl}$) and a steeper post-capping slope (K_c); they also include a faster cyclic deterioration (λ). On average the OMF columns have approximately one-third the rotation capacity of the SMF columns, and the post-capping slope is three times steeper. The joints are also weaker and have decreased deformation capacity due to the lack of transverse reinforcement. The IMF has plastic rotation capacities of approximately one-half those of the SMF.

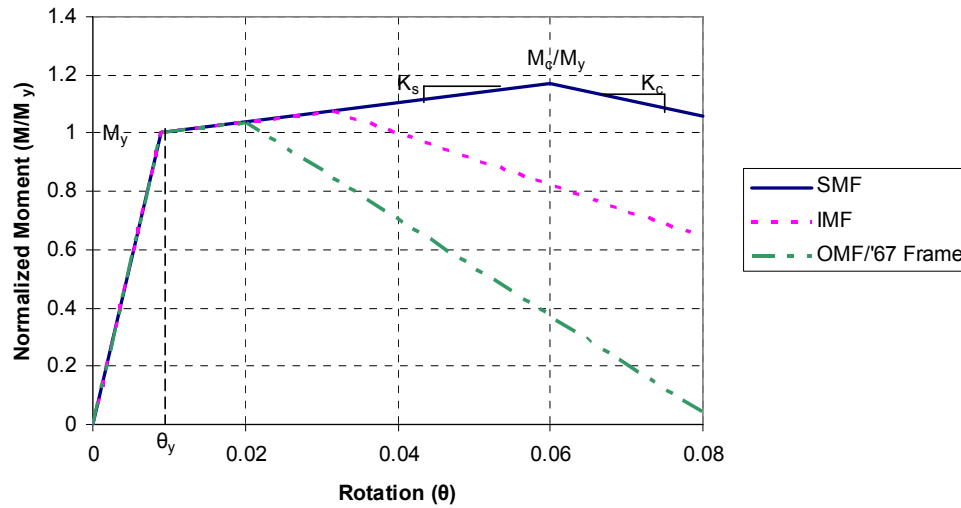


Figure 4. Typical column backbones for each frame structure.

COLLAPSE SIMULATION RESULTS

2003 Special Moment Frame

The results of incremental dynamic analysis for the 2003 SMF are shown in Figure 5. Figure 5a includes the IDA results for both horizontal components from each earthquake record, with a median collapse capacity $S_a(T=1\text{sec})$ of 1.86g. Figure 5b displays only the most damaging component from each pair of horizontal motions. By choosing the horizontal component of the motion that causes collapse first (the “controlling” component), we can roughly approximate the three-dimensional collapse capacity with a two-dimensional analysis. Using this approximation, the median collapse capacity is $S_a(T=1\text{sec}) = 1.56\text{g}$, providing a collapse margin of 1.7 with reference to the MCE of 0.9g. The natural log standard deviation (σ_{ln}) due to variation in ground motions is 0.39. The maximum interstory drift ratio at collapse is between 7 and 12%.

The results of the IDA analysis can be combined in a cumulative distribution function representing the probability of collapse given the ground motion intensity level, as shown in Figure 6. A lognormal distribution is fitted to the empirical collapse data. To account for uncertainties in structural analysis and modeling, additional uncertainty ($\sigma_{ln, Modeling} = 0.45$) is combined (through SRSS) with the record-to-record variation ($\sigma_{ln, RTR} = 0.39$). The additional modeling uncertainty was determined through systematic FOSM analyses to investigate the influence of key modeling parameters (such as uncertainty in component deformation capacity) in the design (Haselton et al. 2007). The added

variability tends to flatten the cumulative collapse distribution (see Figure 6). At MCE = 0.90g, the probability of collapse is 7% without modeling uncertainty and 17% when it is including, demonstrating the important impact that modeling uncertainty has on the collapse prediction. When this collapse distribution is integrated with the hazard curve for the SMF's Los Angeles site, the mean annual frequency (MAF) of collapse for this structure is computed to be 3.5×10^{-4} [collapses/year]. This corresponds to a 2900 year collapse return period.

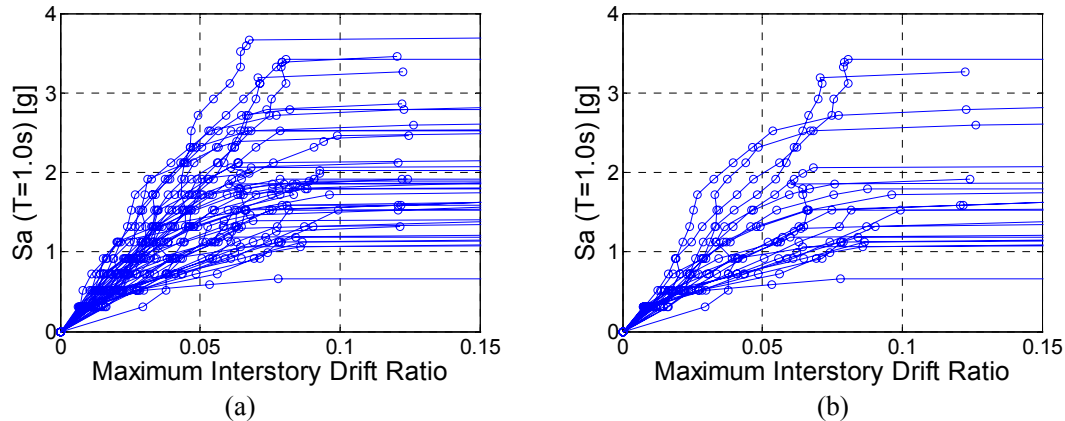


Figure 5. Incremental dynamic results for the SMF for (a) all earthquake components and (b) controlling components only.

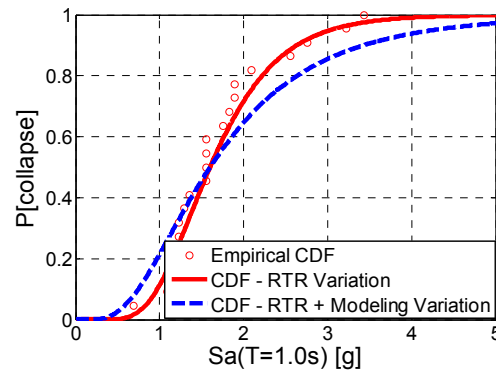


Figure 6. Probability of collapse for SMF, given ground motion intensity level.

As mentioned earlier, the above collapse performance results are based on a general ground motion set that does not account for proper spectral shape (epsilon). This has been shown to be an important aspect of assessing collapse risk (Haselton et al. 2007, Haselton and Baker 2006, Goulet et al. 2006). This paper does not account for the proper spectral shape, so the collapse predictions presented in this paper should be used only for relative comparisons. For example, Goulet et al. (2006) shows that if proper spectral shape is considered for this building, the collapse margin would increase from 1.7 to 2.4. Similarly, the collapse probability and MAF, including modeling uncertainties, would decrease to 3% and 0.7×10^{-4} [collapses/year].

The governing collapse mechanism of the SMF varies for each ground motion, reflecting variations in the frequency content and other characteristics of the ground motion input. The SMF structure tends to fail either in a story mechanism or two-story mechanism involving both beams and columns. While the strong column-weak beam requirement of the 2003 IBC delays the formation of story mechanisms, these analyses indicate that the requirement is insufficient to fully prevent the formation of story mechanisms. (For more detail see Goulet et al., 2007 and Haselton et al. 2007.)

1967 Moment Frame

Figure 7 contains the results of the incremental dynamic analysis for the 1967 moment frame structure for controlling components. The median collapse capacity for controlling components is $S_a(T=1.0\text{sec}) = 0.71\text{g}$, with a computed dispersion of $\sigma_{\ln, \text{RTR}} = 0.30$. These results correspond to a margin of 0.79 compared to the MCE of 0.90g, indicating that the MCE is larger than the median collapse capacity of this structure. The maximum interstory drift at collapse varies between 2.5 and 5 %. The empirical and fitted lognormal cumulative collapse distributions are shown in Figure 8a. Again, modeling uncertainty of $\sigma_{\ln} = 0.45$ is incorporated to account for uncertainties in structural modeling and properties, resulting in a 65% probability of collapse given the MCE. When the collapse CDF is integrated with the hazard curve for the Los Angeles site, the mean annual frequency of collapse for this structure is 32×10^{-4} [collapses/year], corresponding to a 300 year return period. In sidesway, this structure tends to fail in a mechanism involving joints and columns, but the distribution of the mechanism over the height of the structure depends on the ground motion record.

Recalling Table 3, there are several likely failure modes for this structure which have not been directly incorporated into the simulation models. The possibility of column shear failure and subsequent loss of vertical carrying capacity is incorporated through the use of fragility curves defined by Aslani (2005). For each column, these empirically-derived curves define the median and standard deviation of column drift ratio at which shear failure occurs and, subsequently, the column drift ratio at which the column loses its ability to carry gravity loads and collapses vertically. From these relationships it is possible to compute the probability of column shear failure (or loss of vertical carrying capacity) in at least one column, given that sidesway collapse has not occurred at a particular intensity level: $P[C_{\text{other}} | NC_{\text{sim}}, IM = im]$. The total probability of collapse can be computed from the total probability theorem (Aslani 2005, Deierlein and Haselton 2005):

$$P[C | IM] = P[C_{\text{sim}} | IM] + P[C_{\text{other}} | NC_{\text{sim}}, IM]P[NC_{\text{sim}} | IM] \quad (1)$$

where C_{sim} is simulated sidesway collapse, C_{other} is another collapse scenario not directly incorporated in simulation, and NC_{sim} is no sidesway collapse. Equation (1) allows us to consider the effects of column shear failure without directly simulating these complex failure modes; however, the approach neglects interactions between shear and flexural behavior which can affect the structural response predictions, particularly after shear failure occurs in a column.

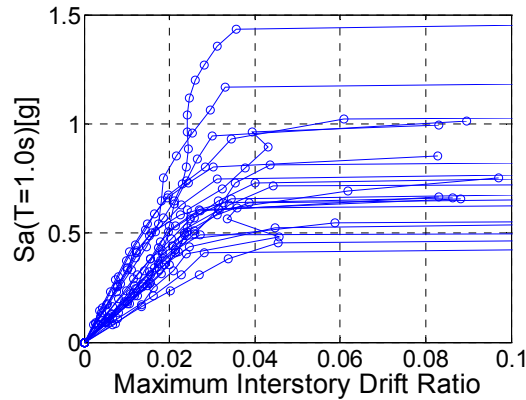


Figure 7. IDA analysis results for 1967 Frame, controlling horizontal components only.

For this frame, fragility functions from Aslani 2005 give a median column drift ratio⁵ of 0.024 corresponding to shear failure of a typical column; the median column drift ratio corresponding to loss of vertical carrying capacity following shear failure is 0.056. When this fragility information is

⁵ Column drift ratio is a measure of deformation in the columns only, whereas interstory drift ratio includes the total deformations in the columns and beams.

combined probabilistically with the IDA analysis through Eq. 1, we obtain Figure 8b, which defines collapse as either sidesway collapse simulated by analysis or shear failure of at least one column. This broader assessment of collapse increases the probability of collapse to 73% at the MCE, and decreases the median collapse S_a to 0.64g. For this structure, inclusion of shear failure has a notable effect, but does not dominate the collapse results. Compared to other older RC frame structures, the high slenderness ratio of the columns makes them relatively less vulnerable to shear failure. Moreover, although shear failure may occur, column loss of vertical carrying capacity following shear failure is very unlikely; the structure will have already collapsed in sidesway (interstory drift ratio between 2.5 and 5%) before columns lose their ability to carry axial load (column drift ratio of 5%).

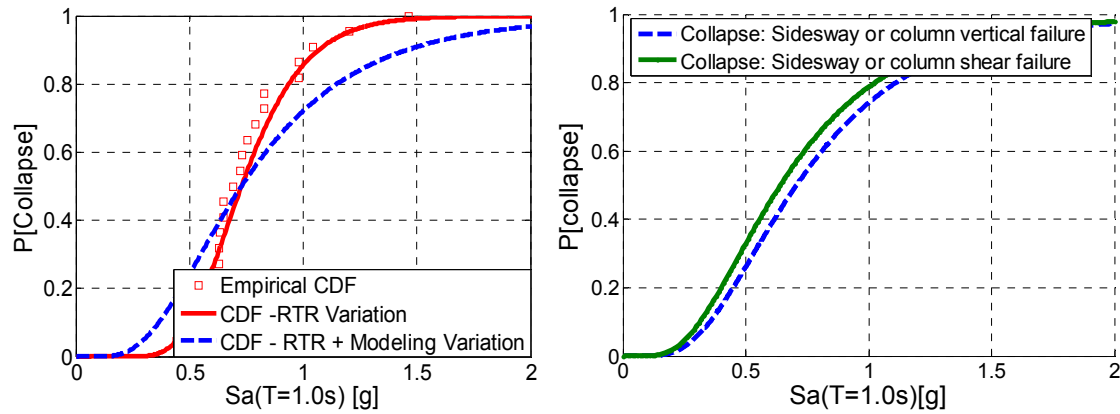


Figure 8. Probability of collapse of 1967 frame given ground motion intensity considering, (a) sidesway collapse only, and (b) sidesway and column shear failure.

2003 Ordinary Moment Frame

The results for the OMF are presented in the same manner as above, with incremental dynamic analysis results shown in Figure 9a. When only the controlling components are considered, the median $S_a(T=1sec)$ at collapse is 0.36g, or approximately 1.9 times the MCE of 0.19g. The maximum interstory drift ratio at collapse ranges from 0.025 to 0.04, indicating this structure's limited deformation capacity. Modeling uncertainty is incorporated in the same manner as above and the resulting probability of collapse for the MCE is 0.12 (including $\sigma_{In,RTR} = 0.36$, $\sigma_{In,Modeling} = 0.45$). As with the 1967 frame there are many possible failure modes besides those sidesway modes directly simulated in the dynamic analysis. Using Equation 1, accounting for vertical collapse corresponding to column LVCC does not change the collapse CDF because sidesway collapse occurs at drifts much smaller than those needed to cause vertical collapse. Just for comparison, if we considered column shear failure to be "collapse," the median $S_a(T = 1sec)$ decreases to 0.33g.

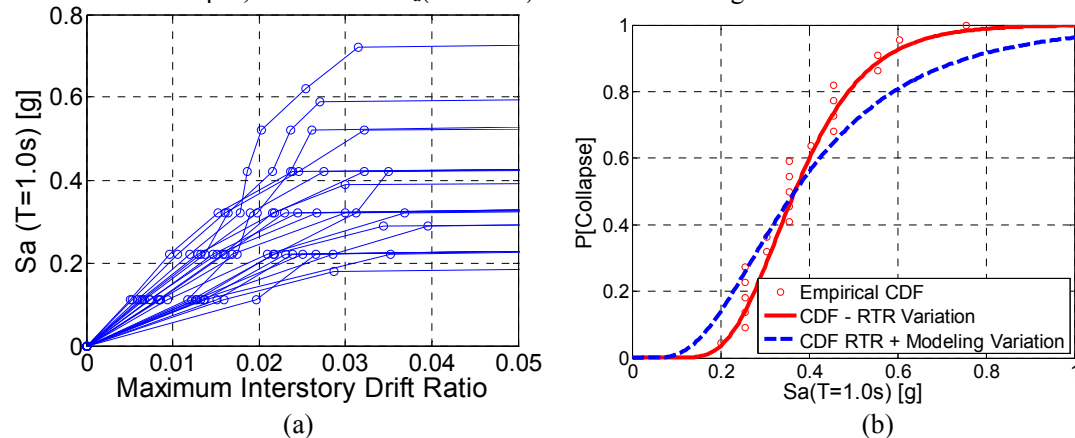


Figure 9. (a) IDA results for OMF, controlling components only, and (b) corresponding cumulative collapse distribution.

2003 Intermediate Moment Frame

Finally, the median collapse capacity for the IMF is 0.51g, considering controlling components as shown in Figure 10. This collapse capacity provides a margin of 1.6 with reference to the MCE of 0.32g. The dispersion is slightly larger in this case, $\sigma_{\ln, RTR} = 0.45$. From Figure 12 we see that the probability of collapse given the MCE is 0.20 including both types of uncertainty. The structure experiences maximum interstory drift ratios at collapse of between 0.04 and 0.06.

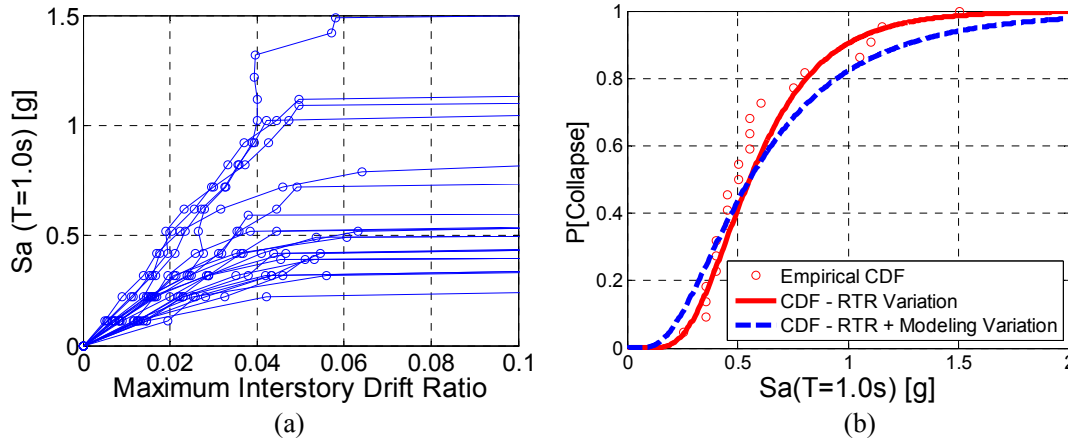


Figure 10. (a) IDA results for IMF, controlling components only, and (b) cumulative collapse distribution for IMF.

COLLAPSE PREVENTION AND RC BUILDING CODES IN THE U.S.

By all measures the new specially detailed reinforced concrete moment frame designed according to the 2003 is safer than the existing 1967 reinforced concrete moment frame. As summarized in Figure 11a and Table 4, the code-conforming structure has approximately twice the collapse capacity (in terms of spectral acceleration) and the mean annual frequency of collapse of the 2003 design is one-tenth of that for the 1967 design. These measurements indicate significant differences in collapse performance in older and new RC frames, despite the fact that the two frames have similar lateral force design requirements (Liel et. al., 2006). The difference in safety reflects the effectiveness of capacity design and detailing requirements of the 2003 provisions, including, the strong column-weak beam requirement, capacity design for shear in beam-columns and joints, and transverse reinforcing bar requirements that provide concrete confinement and inhibit longitudinal rebar buckling. The collapse performance of these two frames, as quantified in Table 4, directly illustrates the combined effect of these provisions in improving the seismic performance of RC frame structures.

As shown in Table 5 and Figure 11b, the current International Building Code provides relatively uniform protection for the three alternative system types (OMF, IMF, and SMF), which are permitted in different seismic regions across the U.S. The consistency in collapse safety is remarkable, considering the large differences in seismic detailing and design requirements. The margin relating the median spectral acceleration to the MCE varies between 1.6 and 1.9, with the OMF the least likely to collapse under MCE ground motions. In absolute terms, however, the different design and detailing requirements for SMF, IMF, and OMF can be clearly seen in the deformation capacities of the structures and the spectral acceleration causing collapse. The interstory drift ratios at collapse of the OMF are similar to the 1967 moment frame, reflecting the similarities in detailing of these two structures, for example in the amount and detailing of column confinement. It should be noted that these collapse analyses were completed as part of the Applied Technology Council Project 63; this project is still in progress, and how these collapse predictions will be utilized in the eventual recommended methodology has not yet been fully determined.

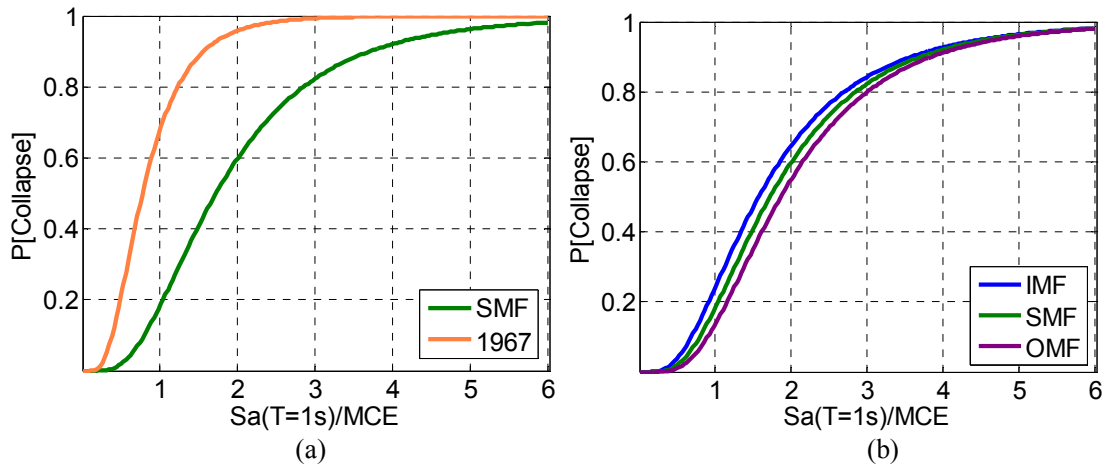


Figure 11. Probability of collapse for different frame structures, where the intensity measure ($S_a(T=1s)$) has been normalized by the MCE. The probability of collapse can be compared for (a) new and older RC frame structures designed for high seismic areas and (b) new special, intermediate and ordinary seismic detailing designed for sites with different seismic hazards.

Table 4. Comparison of collapse safety⁶ for California designs.

Collapse Metrics	2003 SMF	1967 MF
Median Collapse S_a	1.56g	0.71g
Margin : Median Collapse S_a/MCE	1.7	0.8
$\sigma_{in}(\text{total})$	0.60	0.51
$\text{IDR}_{\text{collapse}}$	0.07 - 0.12	0.025 - 0.05
$P[\text{Collapse} \text{MCE}]$	0.17	0.65
$\text{MAF}_{\text{collapse}}$	3.5×10^{-4}	32×10^{-4}

Table 5. Comparison of collapse safety for modern, code-conforming designs with varying levels of detailing.

Collapse Metrics	2003 SMF	2003 IMF	2003 OMF
Median Collapse S_a	1.56g	0.51g	0.36g
Margin : Median Collapse S_a/MCE	1.7	1.6	1.9
$\sigma_{in}(\text{total})$	0.60	0.64	0.58
$\text{IDR}_{\text{collapse}}$	0.07 - 0.12	0.04 - 0.07	0.025 - 0.04
$P[\text{Collapse} \text{MCE}]$	0.17	0.20	0.12

CONCLUSIONS

The ability to quantify collapse safety and deformation capacity at collapse is a product of recent improvements in earthquake engineering tools that enable direct simulation of structures to collapse. These tools provide a series of measures of collapse capacity and, by extension, protection of life safety, which permit a detailed examination of the safety provided by building codes and more transparent decisions in code development. Further work remains to improve and fully validate these tools, including adjustments to reflect spectral shape effects in extreme ground motions, improved quantification of modeling uncertainty, and further calibration of the models to simulate rapid stiffness

⁶ As noted previously, these collapse predictions are based on a ground motion set that does not necessarily represent the correct spectral shape for extremely large (rare) ground motions (see Baker and Cornell, 2006). Adjustments for the spectral shape effect would improve the collapse resistance, more so for the ductile SMF design as compared to the less ductile 1967 and OMF/IMF designs. Work is currently underway by the authors to quantify this beneficial effect of spectral shape for these buildings.

and strength degradation in limited ductility components. Nevertheless, data of the sort presented in this study point to the potential of these methods to evaluate and to help establish appropriate earthquake-resistant design requirements. A modified version of this methodology, with application to a wider variety of buildings, is being developed for a project of the Applied Technology Council (ATC-63: “Quantification of Building System Performance and Response Parameters”) whose aim is to establish a consistent method for evaluating building code design provisions to ensure minimum collapse safety.

ACKNOWLEDGMENTS

This work has been supported in part by the Pacific Earthquake Engineering Research Center through the Earthquake Engineering Research Centers Program of the National Science Foundation (under award number EEC-9701568) and the Applied Technology Council through funding of the ATC-63 project by the Department of Homeland Security's Federal Emergency Management Agency. The authors acknowledge the constructive participation and contributions of collaborators from PEER and ATC in this study. Comments and conclusions made in this study reflect the opinions of the authors and not of any of the sponsors.

REFERENCES

- Aslani, H., 2005. Probabilistic Earthquake Loss Estimation and Loss Disaggregation in Buildings, *Ph.D. Thesis*, Stanford University.
- Baker, J.W. and C.A. Cornell (2006). “Spectral Shape, Epsilon and Record Selection,” *Earthquake Engineering and Structural Dynamics* (in press).
- Deierlein, G., (2004). “Overview of a Comprehensive Framework for Earthquake Performance Assessment, Performance-Based Seismic Design Concepts and Implementation, Proceedings of an International Workshop”, *PEER Report 2004/05*, University of California, Berkeley, 15-26.
- Deierlein, G.G. and C.B. Haselton (2005). “Benchmarking the Collapse Safety of Code-Compliant Reinforced Concrete Moment Frame Building Systems.” *ATC/JSCA US-Japan Workshop on Improvement of Structural Design and Construction Practices, Proceedings of an International Workshop*, Kobe, Japan, October 17-19, 2005.
- Goulet, C., C. B. Haselton, J. Mitrani-Reiser, J. Beck, G.G. Deierlein, K.A. Porter, and J. Stewart, (2006). “Evaluation of the Seismic Performance of a Code-Conforming Reinforced-Concrete Frame Building - from seismic hazard to collapse Safety and Economic Losses”, *Earthquake Engineering and Structural Dynamics*, submitted for review.
- Haselton, C., C. Goulet, J. Mitrani-Reiser, J. Beck, G. Deierlein, K. Porter, J. Stewart, and E. Taciroglu, (2007). “An Assessment to Benchmark the Seismic Performance of a Code-Conforming Reinforced-Concrete Moment-Frame Building”, *PEER Report 2006/xx*, University of California, Berkeley (in preparation).
- Haselton, C.B., A.B. Liel, S. Taylor Lange, and G.G. Deierlein (2006). “Beam-Column Element Model Calibrated for Predicting Flexural Response Leading to Global Collapse of RC Frame Buildings”, *PEER Report 2006/xx*, University of California, Berkeley, (in preparation).
- Ibarra, L.F., R.A. Medina, and H. Krawinkler (2005). “Hysteretic models that incorporate strength and stiffness deterioration,” *Earthquake Engineering and Structural Dynamics*, **34**, 1489 – 1511.
- International Code Council, 2003, *International Building Code*, Falls Church, VA.
- International Conference of Building Officials, 1967. *Uniform Building Code*, Pasadena, CA.
- Liel, A.B., C.B. Haselton, and G.G. Deierlein (2006). “How have changes in building code provisions for reinforced concrete buildings improved seismic safety?”, *8th National Conference on Earthquake Engineering (100th Anniversary Earthquake Conference)*, San Francisco, California, April 18-22, 2006.
- Pacific Earthquake Engineering Research Center, 2006. *Open System for Earthquake Engineering Simulation*, opensees.berkeley.edu; Accessed 6/5/2006.
- Vamvatsikos, D. and C.A. Cornell (2002). “Incremental Dynamic Analysis,” *Earthquake Engineering and Structural Dynamics*, **31**, 491-514.